*34th EPS Conference on Plasma Phys. Warsaw, 2 - 6 July 2007 ECA Vol.**31F**, P-4.065 (2007)*

Verification of the CAS3D-perturbed equilibrium code in the cylindrical limit

C. Nührenberg[1], S.R. Hudson[2], A.H. Boozer[3]

[1] *IPP, EURATOM Association, Wendelsteinstr. 1, 17491 Greifswald, Germany*

[2] *PPPL, Princeton NJ 08543, USA*

[3] *Columbia University, New York NY 10027, USA*

1 Perturbed equilibria

A numerical computation of an ideal MHD equilibrium may suffer from the following short-comings. In the tokamak case, an axisymmetric Grad-Shafranov solver is not suitable if error-fields turn the 2d into a 3d problem. In the stellarator case, equilibria are usually calculated numerically using the assumption of integrability, or nested magnetic surfaces, as it is done for example in the VMEC code [1]. In many applications, especially for plasma configurations optimized for good magnetic surfaces, this is a sufficient approximation. If, however, the island structure of the magnetic field is expected to be important [2], such as in a stellarator or in a tokamak with some error field, then numerical tools that calculate the global equilibrium without the assumption of nested magnetic surfaces, such as the PIES code [3], are employed. These calculations are not only computationally intensive, the presence of rational surfaces implies that 3D MHD equilibria with smooth pressure profiles do not in general exist [4]. To compute 3D ideal MHD equilibria, one needs to carefully account for the singularities, and discontinuites, that arise at rational surfaces. A rigorous mathematical treatment of a perturbed equilibrium is provided by linear ideal stability theory [5] which determines the plasma response to small perturbations. This approach has been implemented in the CAS3D stability code [6], which is used here.

$$\delta W = \delta^1 W + \delta^2 W$$

$$\delta W = \int (\nabla p - \vec{\jmath}\times\vec{B})\cdot\vec{\xi}\,\mathrm{d}^3 r - \frac{1}{2}\int \vec{\xi}\cdot\mathscr{F}\left[\vec{\xi}\right]\mathrm{d}^3 r \qquad (1)$$

$$\delta^1 W = \int \xi^s \left\{(p' - p'_{\mathrm{new}}) + \vec{B}\cdot\nabla(\widetilde{\beta}_{\mathrm{mde}} - \widetilde{\beta}_{\mathrm{metric}})\right\}\mathrm{d}^3 r \qquad (2)$$

$$\delta^2 W = \frac{1}{2}\int \left\{\left|\vec{B}_1 + \frac{\vec{\jmath}\times\nabla s}{|\nabla s|^2}\xi^s\right|^2 + \gamma p(\nabla\cdot\vec{\xi})^2 - \mathscr{A}(\xi^s)^2\right\}\mathrm{d}^3 r \qquad (3)$$

2 Ideal MHD energy principle

The ideal MHD equilibrium equation is $\nabla p = \vec{\jmath}\times\vec{B}$, with the scalar pressure $\nabla p = p'\nabla s$ a surface function. In Eq. (1), the first term describes the departure from an equilibrium state, the second term, $\delta^2 W$, is given by the ideal MHD force operator $\mathscr{F}$. The notation used below may be found in Refs. [6]. In magnetic coordinates, the magnetic field may be written as $\vec{B} = I\nabla\phi + J\nabla\theta + \widetilde{\beta}\nabla s$ and $\sqrt{g}\vec{B} = -F'_{\mathrm{T}}\vec{r}_{,\phi} - F'_{\mathrm{P}}\vec{r}_{,\theta}$, with I and J the currents and F_{P} and F_{T} the fluxes. The covariant component $\widetilde{\beta}$ may be determined from the metric coefficients as $\sqrt{g}\widetilde{\beta}_{\mathrm{metric}} = F'_{\mathrm{T}} g_{s\phi} + F'_{\mathrm{P}} g_{s\theta}$. The scalar analog of the MHD equilibrium equation in magnetic coordinates gives rise to the magnetic differential equation

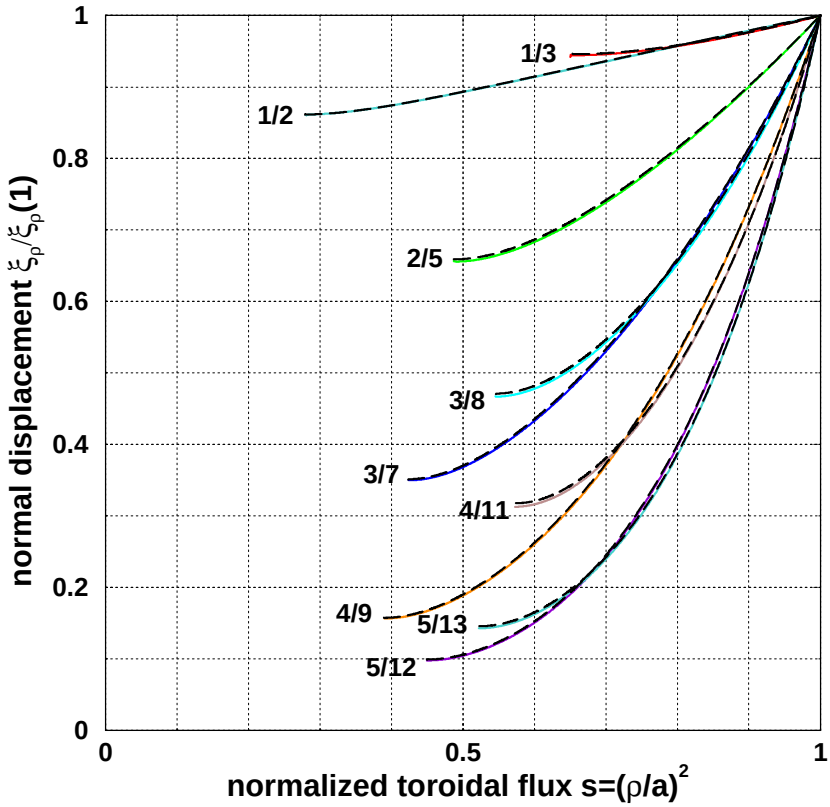

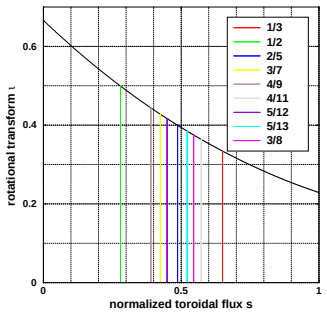

Figure 1: Top: Rotational transform in an $A = 10$ zero-β cylinder configuration. Rational ι-values are indicated. Left: Normal displacements versus normalized toroidal flux: Comparison of results given by a cylinder-code (black dashed lines) and the CAS3D code (coloured).

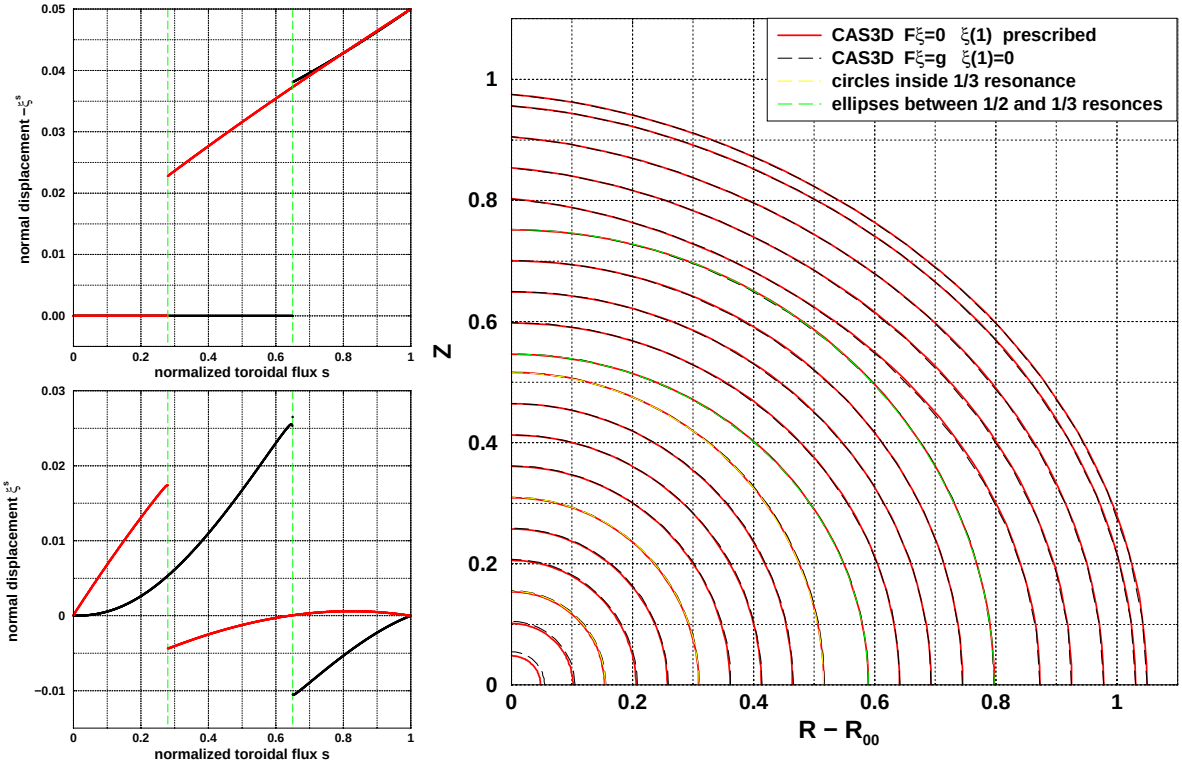

Figure 2: Left: Normal displacement harmonics with jumps at resonances $\iota = 1/2$ (red) and $1/3$ (black); top: unperturbed case with perturbation prescribed on boundary; bottom: perturbed case with fixed-boundary perturbation. Right: Quarter of cross-section with the surfaces including the perturbation. Inside the innermost resonance ($R - R_{00} \lesssim 0.52$) the surfaces are circles due to the shielding; inside $0.52 \lesssim R - R_{00} \lesssim 0.8$ they are ellipses.

$\sqrt{g}\vec{B}\cdot\nabla\widetilde{\beta}_{\mathrm{mde}} = p'(\sqrt{g}-V')$. In equilibrium $\widetilde{\beta}_{\mathrm{metric}} = \widetilde{\beta}_{\mathrm{mde}}$. The second term in Eq. (2) describes the departure of a given set of magnetic surfaces, determining $\widetilde{\beta}_{\mathrm{metric}}$, from the equilibrium, described by $\widetilde{\beta}_{\mathrm{mde}}$. If the plasma-pressure is slightly changed, then the first term in Eq. (2) also contributes. In Eqs. (1) to (3), $\vec{\xi}$ is the MHD displacement vector, and $\xi^s = \vec{\xi}\cdot\nabla s$ the normal displacement. In the CAS3D stability code, by means of a Galerkin method, Eqs. (1) to (3) are recast as a system of linear equations, with the matrix given by Eq. (3) and the right hand side by Eq. (2). In a perfect equilibrium, the right hand side vanishes, and the homogeneous problem is solved. The solution is non-trivial only if inhomogeneous boundary conditions are used. An inhomogeneous boundary condition for the normal displacement corresponds to applying an error-field on the boundary, $\vec{B}_1\cdot\nabla s = \vec{B}_0\cdot\nabla\xi^s$; the plasma boundary will be perturbed. A homogeneous boundary condition means that a fixed-boundary perturbation is used; the plasma boundary stays as prescribed. The normal displacement ξ^s appears in the computation of the perturbed surfaces, $\vec{r}_1 = \vec{r}_0 + (\vec{\xi}\cdot\vec{n})\vec{n}$, with $\vec{n}$ the outer unit normal.
Resonant error-fields may produce magnetic islands if the corresponding rational surface is inside the plasma. In ideal MHD magnetic islands may be characterized by a surface current, which prevents an island from opening at the rational surface. The strength of the surface current is related to a discontinuity allowed in the resonant normal displacement, ξ^s. The strength of the surface current is related to the width of the island [5].

3 Discontinuous normal displacement in a cylinder

As part of code validation, the influence of error fields has been studied in cylindrical geometry, for an equilibrium with aspect-ratio A=10, vanishing plasma-β, and rotational-transform $0.66 > \iota > 0.23$ (compare Fig. 1). The CAS3D results have been benchmarked with a code for the ideal cylindrical stability [7]. In this code the exterior tearing equation, with singular points at the rationals and the origin, has been implemented using a shooting and matching technique. The result of the benchmark is shown in the left frame of Fig. 1. The nine normal displacement harmonics that have been studied coincide to a very good approximation. From the plasma boundary the error-field harmonics decay and are completely shielded off by the respective rational surfaces. Since in a cylinder all perturbation harmonics decouple, they are not influenced by the other rational surfaces.
Prescribing a finite normal displacement in the perfect equilibrium case (homogeneous problem with inhomogeneous boundary conditions) is equivalent to using a vanishing normal displacement in a correspondingly deformed plasma state. For a check of this statement, two of the rational ι-values of the above benchmark have been studied, $1/2$ (at $s = 0.28$) and $1/3$ (at $s = 0.65$). If the perfect cylinder equilibrium is perturbed with a small $\vec{B}_1$ on the plasma boundary, then the respective normal displacement harmonics are discontinuous at the respective resonant surfaces. The top left frame of Fig. 2 shows the corresponding CAS3D result, a subset of the above-described benchmark calculation. In a second calculation an equivalently helically distorted equilibrium was studied, being described by a VMEC equilibrium, which is approximate near the resonances. In this calculation the second term in Eq. (2) is the driving term g in

the inhomogeneous problem with homogeneous boundary conditions. The bottom left frame of Fig. 2 shows the resonant normal displacement harmonics vanishing on the plasma boundary which represent the first order correction leading to a *better* equilibrium. For the $m = 3(2)$, $n = 1$ harmonic, the magnitude of the jump, $|\xi^s_{mn+} - \xi^s_{mn-}|$, is 0.038 (0.023) in the $\mathscr{F}\vec{\xi} = 0$ calculation as compared to 0.036 (0.022) in the $\mathscr{F}\vec{\xi} = g$ case. To see whether the two calculations lead to the same result, the shifted surfaces, $\vec{r}_1 = \vec{r}_0 + (\vec{\xi}\cdot\vec{n})\vec{n}$, have been determined (see the right frame in Fig. 2). Black dashed lines are for the $\mathscr{F}\vec{\xi} = g$ calculation, red lines for the $\mathscr{F}\vec{\xi} = 0$ calculation. The two sets of lines coincide to a very good approximation. Outside the resonance closest to the plasma boundary, here $\iota = 1/3$, the surfaces are deformed according to the $m = 2,3$ $n = 1$ perturbation. Between the two resonances, the surfaces are ellipses: The $\iota = 1/3$ resonance screens off the $m = 3$ perturbation, the $m = 2$ perturbation remains. Inside the resonant surface closest to the magnetic axis, here $\iota = 1/2$, the surfaces are circles, which demonstrates the complete shielding of the two resonances.

4 Plasma-pressure change in a stellarator

As discussed in Secs. 1 and 2, the perturbed equilibrium concept can also be used to find the response of the plasma to a small plasma-pressure change. The first term in Eq. 2 then describes how the deviation in pressure gradient contributes in the determination of the corresponding normal displacement. As an application, the effect on the equilibrium due to an increase in volume-averaged plasma-β, from $\langle\beta\rangle = 0.045$ to 0.048, has been studied for a high-mirror W7-X variant, maintaining a fixed rotational-transform profile. A first calculation has been restricted to normal displacement harmonics with poloidal node number $m = 1$, and toroidal node numbers $n = -10,-5,0,5,10$. The results of this calculation are shown in Fig. 3. The CAS3D ($+$ in the right frame) and VMEC ($\times$) results are compared on two outboard symmetry lines: on the bean-shaped cross-section (cross-section half-width ≈ 0.2 m, black symbols) and on the triangular cross-section (≈ 0.7 m, red symbols).

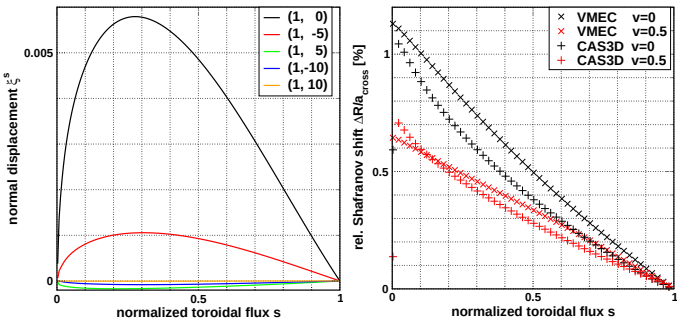

Figure 3: Left frame: Normal displacement harmonics describing the perturbation of a W7-X variant from $\langle\beta\rangle = 0.045$ to 0.048. Only $m = 1$ harmonics have been studied. Right frame: The enhanced Shafranov shift for the normal displacement in the left frame, normalized to the respective cross-section half-width, ≈ 0.2 m at the bean-shaped cross-section, black symbols, ≈ 0.7 m at the triangle, red symbols.

•[1] S.P. Hirshman, W.I. van Rij, and P. Merkel, Comput. Phys. Commun. **43** , 143 (1986). •[2] S.R. Hudson *et al.*, Phys. Rev. Lett. **89**, 275003 (2002). •[3] A. Reiman and A.H. Greenside, Comput. Phys. Commun. **43** , 157 (1986). •[4] H. Grad, Phys. Fluids **10**, 137 (1967). S.R. Hudson *et al.*, Phys. Plasmas **14**, 052505, (2007). •[5] A.H. Boozer, Phys. Plasmas **6** (3), 831 (1999). — C. Nührenberg and A.H. Boozer, Phys. Plasmas **10** (7), 2840 (2003). — A.H. Boozer and C. Nührenberg, Phys. Plasmas **13**, 102501 (2006). •[6] C. Schwab, Phys. Fluids B **5** (9), 3195 (1993). — C. Nührenberg, Phys. Plasmas **3** (6), 2401 (1996). — C. Nührenberg, Phys. Plasmas **6** (1), 137 (1999). •[7] S.R. Hudson, priv. comm. •